Research article

VADOCHARGE-N: a Vadose Flow and N-Transport Simulation Model for the Northern Guam Lens Aquifer

Nathan C. Habana[1, 3, *], Jonathan L. Salvacion[2], John W. Jenson[3], Joseph D. Rouse[3]

[1]Environmental Engineering, PhD, Graduate Studies Program,
[2]Graduate Studies Office, School of Graduate Studies,
Mapúa Institute of Technology, Intramuros, Manila, Philippines www.mapua.edu.ph
jlsalvacion@mapua.edu.ph
+63-2-527-3681

[3]Water Environmental Research Institute of the Western Pacific,
University of Guam, Mangilao, Guam, Territory USA www.weriguam.org
*nchabana@uguamlive.uog.edu, jjenson@uguam.uog.edu, jdrouse@uguam.uog.edu
+1-671-735-2685, fax: +1-671-734-8890

ABSTRACT

The 60-180 m thick limestone bedrock vadose zone of the Northern Guam Lens Aquifer (NGLA) presents special challenges for modeling vadose flow and transport. In particular, the need to account for both slow percolation of infiltrating rainwater (spanning months) and fast flow from ponded storm waters (requiring only hours or minutes) to the water table led to the development of an analogue recharge model, VADOCHARGE [8,9]. VADOCHARGE adapted the USACE *Streamflow Synthesis and Reservoir Regulation* watershed and router model to each cell of an underlain finite element groundwater model mesh, to estimate meteoric recharge flux at the water table. VADOCHARGE-N incorporates algorithms to model the transport and transformation of nitrogen (N) species, based on a selected subsurface N-cycle model for the NGLA. Components include a wastewater discharge model by the Box-Muller transformation algorithm to calculate synthetic discharge of gray water volume, Kjeldahl N, and dissolved oxygen (DO). The N species undergo virtual simultaneous transformations based on a biogeochemical transport conceptual model. The numerical implementation uses chemical and Monod kinetics to simulate nitrification-denitrification reactions in the percolating ("slow-flow") component. The model thus produces realistic N transport that may be coupled to an underlying phreatic solute transport model. The results may provide water resource management insight into optimum development and appropriate protective measures.

Keywords: SSARR hydrologic vadose analogue model, intercept and soil moisture model, deep karst vadose flow, recharge and evapotranspiration, wastewater nitrogen fate and transport

1. INTRODUCTION

Unconfined karst aquifers such as the Northern Guam Lens Aquifer (NGLA) are uniquely vulnerable to domestic wastewater discharge. Karst aquifers typically have fractures, conduits, and cavern sized voids that may facilitate domestic wastewater discharge, particularly in conjuction with the flow of meteoric waters. The complex spatial distribution of porosity and hydraulic conductivity in karst aquifers present special challenges to modelers [4, 9, 10, 32]. The thick vadose zone of the NGLA (60-180 m amsl) contains a variety of flow paths, to that there may be substantial ranges in time-lag and attenuation along multiple flow paths. Moreover, different paths may activate according to storm intensities. Such challenges have made it difficult to model vadose flow [4]. Studies of aquifer response to rainfall, however, reveal a similarity to surface flows [4,9], which suggested the application of an analogue model to apply a suface reservoir storage and flow algorithm to vadose storage and flow. VADOCHARGE [8, 9] applies US Army Corps of Engineers Flood-Runoff Analyis Model [38] algorithm to account for the contributions of both slow percolation through the aquifer matrix, which can take up to 20 months [18], and vadose fast flow, which may take only hours or even minutes [4, 6, 8, 13, 18]. This paper reports on the development VADOCHARGE-N, designed to simulate the flow and transport of N from domestic discharge. VADOCHARGE-N incorporates an algorithm for the subsurface nitrogen cycle to simulate the transformation nitrogen species and calculate the N species transport resulting from the percolation and fast flow of meteoric waters. The model is meant to be coupled to an underlain numerical phreatic solute transport model. It will eventually be coupled to and tested with a phreatic model to help predict the contribution of domestic discharge to the amount of N in drinking water.

2. AQUIFER CHARACTERISTICS

Guam is the southernmost and largest of the Mariana Islands [37]. The southern half is formed of volcanic mountains cut by stream and river valleys. The northern half is an uplifted and slightly tilted limestone plateau, which comprises the NGLA, designated a sole-source aquifer by the USEPA [41], and supplies 80% of Guam's drinking water.

2.1. General Hydrology and Hydrogeology

Guam has a rainy season (July to December) and dry season (January to June). The average annual rainfall is 250 cm, distributed as 175 cm (70%) and 75 cm (30%) across the rainy season and dry season, respectively. Guam has high interannual rainfall variability related to ENSO; prolonged and extended dryness typically occurs during the year following El Nino [19, 20, 30]. A nearly complete archive of daily rainfall data for Guam is available from the National Climatic Data Center [27].

In terms of the Carbonate Island Karst Model [26], Guam is a composite island, so that the NGLA is partitioned into semi-contiguous basins by the basement rock, which rises not only above sea level but to a limited extent above the plateau surface as well. The core unit of the aquifer is the Miocene-Pliocene Barrigada Limestone, a detrital foraminiferal limestone deposited in a deep to shallowing bank environment. The texture of the Barrigada Limestone varies from soft and friable to firm and massive. Structural modification and a complex history differential tectonic uplift and subsidence overprinted by eustatic sea-level variations has produced a complex eogenetic [43] triple-porosity karst [25], with matrix, fracture, conduit porosity [14, 47]. The distribution of porosity is difficult to predict, especially at the local scale. An appropriate representative elementary volume [2] is therefore difficult to determine [16]. Local hydraulic conductivities may be between 80-2000 m/d and regionally up to 15,000 m/d [12, 13, 32].

2.2. N Biogeochemistry

Nitrogen is a well known component of sewage. Consumption of certain levels of nitrite and nitrate are a health threat, which may cause methemoglobinemia, cyanosis, or "blue baby" syndrome, affecting blood iron capacity to acquire oxygen, which may be fatal in excessive amounts [24, 28]. Moreover, nitrogen species can be indicators of more general sewage contamination. Nitrogen biogeochemistry is known to be complex and sensitive to environmental conditions, including temperature, humidity, and pH. Temperature and humidity are relatively constant in the tropical climate of Guam, but pH can vary significantly in karst aquifers. The N biogeochemistry incorporated in VADOCHARGE-N relies on [15, 42] as well as experimental work to estimate the chemical evolution (fates) of the various N species (organic nitrogen, ammonia, nitrite, and nitrate) during transport through the thick vadose zone of the NGLA.

Undiluted influent to a septic tank or sewer main system, sometimes referred as "black water," is often loaded with Kjeldahl N (ammonia-N and organic-N). Upon sitting in transitional containment, usually under anaerobic conditions, the organic-N may undergo deamination and ammonification to yield ammonia-N. Anaerobic conditions hamper nitrification, thus effluents are often low in nitrates. Leaving its transitional containment as effluent or even raw sewage, as domestic discharge into the aquifer by leaks or spills, the wastewater may gain dissolved oxygen, DO, by aeration during percolation. Daily discharge effluent concentrations may be random and also have a form of distribution, [3] assumed here normal. The presence of DO promotes oxidation of ammonia-N to nitrite, then nitrate, referred to as nitrification. Percolation may play an important role; when it slows or ceases, producing stagnant or "water-logged" conditions, the DO can be consumed by nitrification, so that denitrification ensues [21, 22], in which nitrates become a source of oxygen for denitrifiers. Also, in that condition, ammonification continues and nitrification ceases. If percolation continues to maintain aeration, however, then the ammonia-N may be nitrified throughout its transport, and nitrate-N may reach the water table, with enough moisture. Denitrification prevails in anaerobic conditions ideally less than 0.2 ppm [1, 3]. The high porosity and abundance of large pore spaces in the limestone bedrock of the NGLA suggest that vadose waters will most likely experience the latter rather than the former conditions.

3. METHODS - MODEL CONFIGURATION

The VADOCHARGE-N computer program is designed according to its conceptual, mathematical, and numerical model configurations. This paper emphasizes on the numerical model. The term *node-shed* refers to a finite element node cell sized surface watershed and vadose column that extends to an underlain phreatic model mesh [8,9].

3.1. Conceptual Models

As noted above, karst aquifers present special challenges for modelers. Conceptual models [cf., 29, 45, 47] note that even among karst aquifers the relative contributions of matrix, fracture, and conduit porosity can vary, to there is not even a single "one-size-fits-all" conceptual model for karst aquifers. Nevertheless, certain simplifications allow modeling selected properties. For the NGLA, in which recharge has been observed to be divided between slow percolation and fast flow, it suffices to incorporate these two processes to model water flow and contaminant transport through the vadose zone. VADOCHARGE-N extends the surface infiltration and vadose flow model VADOCHARGE [8], to incorporate not only meteoric waters but also wastewater bulk flows and transport of N constituents. Time distribution for input pulses are achieved through application of the *Streamflow Synthesis and Reservoir Regulation* (SSARR) routing technique developed by the USACE for modeling of surface reservoir storage and flow [33, 38, 39]. This application is based on the observation that water-table hydrographs along concentrated flow routes in the NGLA [4, 8] are analogous to surface stream hydrographs. Vadose flows through large pores (fractures and conduits) reflect the same-shaped ephemeral spikes and recovery curves as in surface stream hydrographs. Similarly, slow percolation through the matrix of the vadose zone is analogous to percolating base flow into and out of surface streams, reflecting similar lag times and attenuations and producing analogous curves. Application of the antecedent model, VADOCHARGE [8] to simulate flow in the NGLA have demonstrated the utility of the SSARR as conceptual model for vadose flow in this type of aquifer.

Figure 1 illustrates the concept for two possible scenarios as the fate and transport of N in effluent discharge. As described in the biogeochemistry, presence of DO plays an important role in triggering nitrification and denitrification. Scenario 1 is the case where DO is consumed from nitrification and never regained as it percolates within an arbitrary depth, denitrification removes nitrates. Scenario 2 is continuous gain of DO as the effluent percolates, as a case with Cowan's lysimeter experiment [5], nitrification prevails.
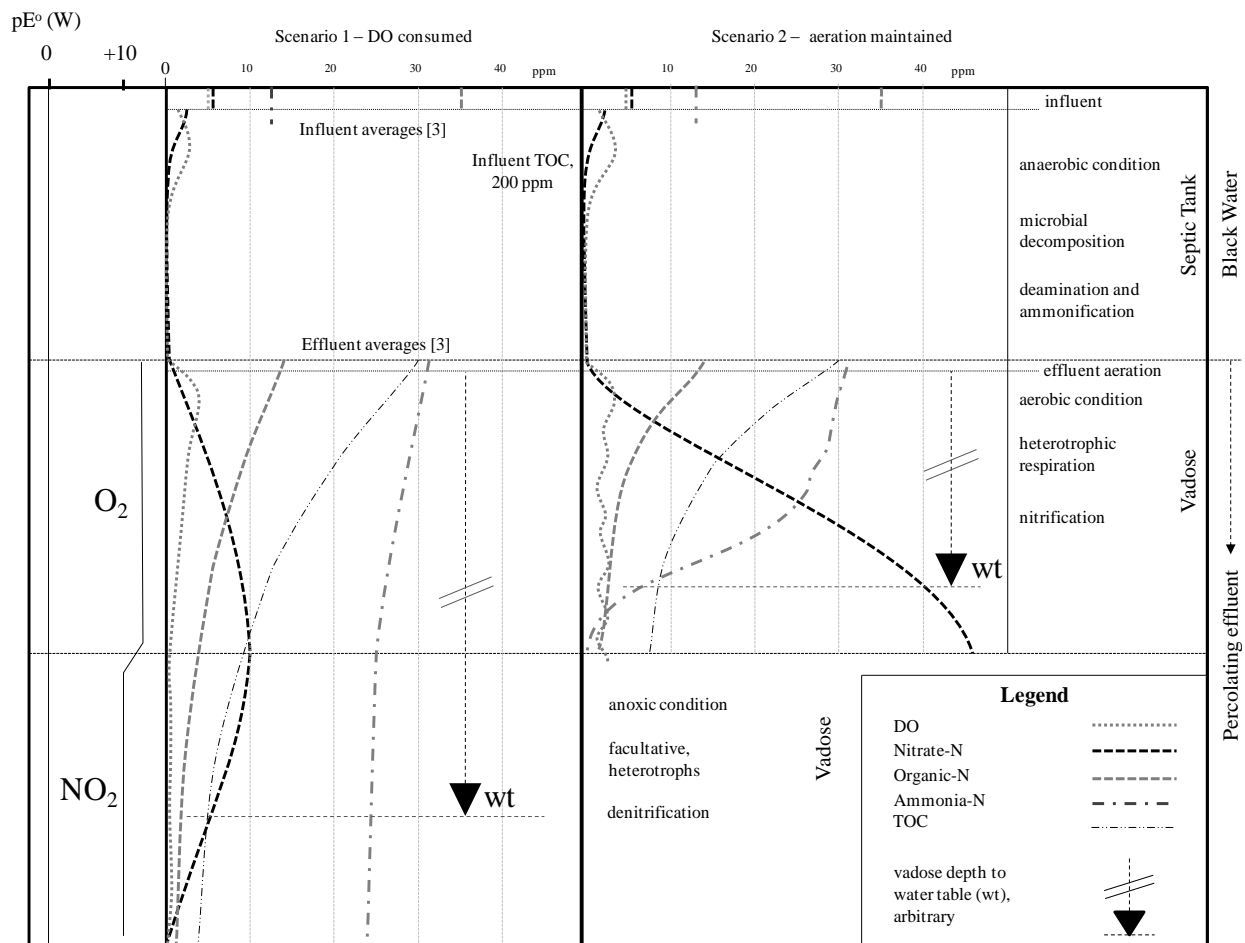
Figure 1. Conceptual model for transport and fate of effluent N through deep karst. Scenario 1 shows oxygen is consumed before it reaches the water table would pivot denitrification in the vadose. Scenario 2 shows oxygen is gained as it percolates, maintaining nitrification phase, limited by available convertible ammonia-N. Adapted from [42].

3.2. Mathematical Models

Hydrologic watershed and streamflow type models are based on the continuity equation of the form $dS/dt = I - O$, where dS/dt is the time rate of change of a system water storage, I is the water input to storage, and O is storage water output. The system generally refers to particular models here that have capacity to hold water, specifically defined for each model and derived into a water balance or accounting model. The discharge of wastewater volume and Kjeldahl N and DO concentrations are synthetic values of random and normal distribution, using a Gauss Deviation method application of the Box-Muller Transformation algorithm [7, 31]. The vadose water transfer applies hydrologic routing, derived from the average form of the continuity equation. Chemical N transformation applies 0th and 1st order chemical kinetics and sorption using Monod kinetics as Langmuir isotherms [15, 42].

3.3. Stage1: Interception, Soil Moisture, and Discharge Synthesis, Numerical Models

Stage 1 applies the continuity equation to account for rainfall interception and soil moisture change. The continuity equation is configured into an iterative current water content balance equation $S_2 = S_1 + I_2 - O_2$, where S is *system storage* and I and O are *input* and *output* volumes respectively. Input and output are conditional of water containment capacity and potential evaporation relationships. Time discretization Δt is daily, and subscripts of the following numerical model solutions refer to time periods 1 and 2, previous and current day, respectively.

3.3.1. Intercept model

Intercept is a process, modeled with land cover feature, a new and unique attribute of the node-shed polygon zone [8, 9, 34, 35], of vegetal or impervious surface that may capture a certain amount of rainfall. The water balance equation is redefined as intercept storage *IS* and the input as rainfall.

$$IS_2 = \underset{i}{\underline{IS_1 + I_2}} - O_2, \quad let\ I_2 = R_2, \quad i = IS_1 + R \qquad \text{Eq. 1}$$

Equation 1 introduces an intermediate condition, *i*, to determine the intermediate intercept *INT* in Eq. 2. Input to storage is limited by a specified intercept capacity *IC* and excess rainfall *XSM* is input to the underlain soil moisture model.

$$INT_2 = \begin{cases} IC & | \ i > IC, \quad XSM_2 = i - IC \\ i & | \ 0 \le i \le IC, \quad XSM_2 = 0 \end{cases} \qquad \text{Eq. 2}$$

INT is further reduced by output from surface evaporation of intercepted moisture. Pan evaporation, *P*, as potential evaporation, is compared with intercepted moisture to determine the quantity of output to reduce the intercept storage from Eq. 2. *IE* is recorded daily surface evaporation from intercept:

$$O_2 = \begin{cases} INT_2 & | \ P_2 > INT_2 \\ P_2 & | \ P_2 \le INT_2 \end{cases}, \quad IE_2 = O_2 \qquad \text{Eq. 3}$$

3.3.2. Soil moisture model

The soil moisture model is similar to the intercept model as it also applies the moisture balance equation. *SM* is the soil moisture storage in the equation $SM_2 = SM_1 + I_2 - O_2$. The input is *XSM* in Eq. 2, computed from either Eq. 2 or direct rainfall input (no intercept), infiltration of the surrounding land surface for each respective zone. The intermediate soil moisture input is *smi*:

$$SM_2 = \underset{smi}{\underline{SM_1 + I_2}} - O_2, \quad I_2 = XSM_2\ or\ R_2, \quad smi = SM_1 + XSM_2 \qquad \text{Eq. 4}$$

The *smi* is compared to the soil moisture threshold or field capacity, *FC*, to determine the intermediate soil moisture input, *SMI*, in Eq. 5:

$$SMI_2 = \begin{cases} FC & | \ smi > FC, \quad XRE_2 = SMI_2 - FC \\ smi & | \ smi \le FC, \quad XRE_2 = 0 \end{cases} \qquad \text{Eq. 5}$$

XRE is moisture that will move to Stage 2, as excess moisture is gravitated past the soil when *smi* is greater than *FC*. This is the recharge-reduced soil moisture. Current *SMI* is further reduced by evapotranspiration, *ET*. *ET* is calculated where the surface zone of a node-shed is vegetated:

$$SM_2 = SMI_2 - O_2, \quad SM_2 = SMI_2 - ET_2 \qquad \text{Eq. 6}$$

The computation of *ET* uses an evapotranspiration curve model, Fig. 2. This curve has 3 optional model settings, based on Viemeyer, Pierce, or Thornthwaite [44]. The x-axis is the recharge-reduced *SM* in Eq. 5, and *FC* ratio for a particular soil type in the zone polygon. The curve models determine the percent of pan evaporation factor, *ETP*, multiplied to *P* to determine *ET*, soil moisture output, Eq. 7.

$$ET_2 = P_2 \cdot ETP_{(SMI_2\ /\ FC)} \qquad \text{Eq. 7}$$

The computations are solved for each zone area of a node-shed for all node-sheds in the entire model domain. The daily value of moisture to recharge for a given node-shed is optionally the sum of zone recharge or zone area-weighted average recharge as bulk moisture that moves into the router. The node-shed bulk recharge is split analogous to SSARR splitting of runoff and subsurface flow [39].

3.3.3. Wastewater, Kjeldahl N, and DO discharge model

The daily effluent volume rates, the Kjeldahl N, and DO concentrations from sources (mostly residences and workplace buildings) must be estimated by some realistic means. Domestic sewage discharge outputs, in terms of long term daily discharge rates and concentrations from source buildings are thus assumed to be random and normally distributed. For VADOCHARGE-N, wastewater volume, Kjeldahl N, and DO are determined using the Box-Muller Transformation (BMT) algorithm, a Gauss deviation method [31]. The BMT algorithm produces

normally distributed random values about a specified range of low and high values in a histogram analysis. The wastewater and constituents, of a source specified node-shed, thus determined from the BMT algorithm are assigned to the wastewater router in Stage 2.
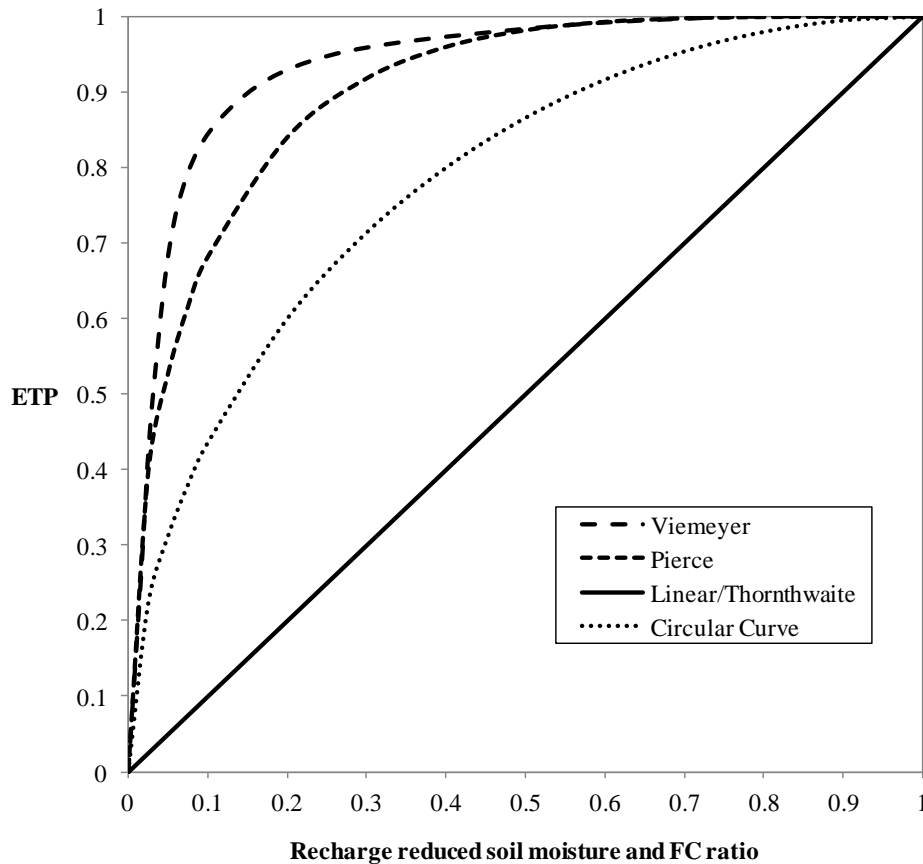
Figure 2. Evapotranspiration factor curve models. Adapted from [44].

3.4. Stage 2: SSARR Moisture Routing, Numerical Model

Hydrologic routing is derived from the central difference or averaged form of the continuity equation [38], $S_2 - S_1 = t(\bar{I} - \bar{O})$. The S, I, and O are renewed and redefined hereafter for the derivation of routing method in Stage 2.

SSARR routing is a surface hydrologic technique for producing hydrographs, a version of the Modified Puls [38], arranged and depicted as the method of cascading weirs [39]. Each *storage period*, S, is assumed to have a linear relationship to *output periods, O*, respectively, which introduces a *time-in-storage* parameter, Ts, thus $S = Ts \cdot O$. This is substituted in the continuity equation above, forming $T_s O_2 - T_s O_1 = t(\bar{I} - \bar{O})$ and algebraically solved for the current output, Eq. 8. C is a time constant for a time in storage parameter T_s (hours) and time period t ($t = 24$ hrs).

$$O_2 = \left(\bar{I} - O_1\right)C + O_1, \quad C = \frac{t}{\left(T_s + t/2\right)} \qquad \text{Eq. 8}$$

Equation 8 solves the current output in the *Method of Cascading Weirs* [39]. For vadose flow the analogue is depicted as a vertical series of water storage cells, transferring vadose groundwater from one cell to another, Fig. 3. The result of this algorithm is the distribution of recharge to the water table over time, producing a hydrograph. *Ts* control the attenuation and the number of cells in the series provide lag.

The diagram depicts the cell phase moisture transfer with the following equations:

$$\Delta S = S_2 - S_1 = \overline{I} - \overline{O}$$

$$S_1$$

$$+\Delta S$$
$$-\Delta S$$

$$S_2 = S_1 + \Delta S$$

$$\overline{I} = \frac{(I_1 + I_2)}{2}$$

$$O_2 = (\overline{I} + O_1)C + O_1$$

$$\overline{O} = \frac{O_1 + O_2}{2}$$

$$\overline{I} = \overline{O}$$
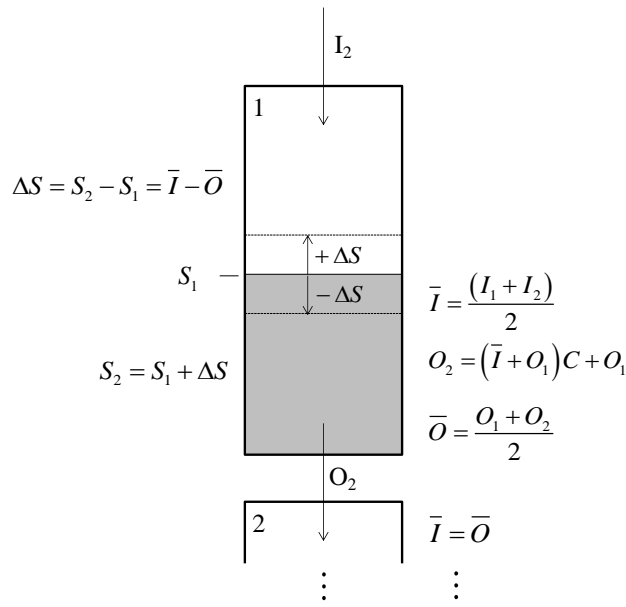
Figure 3. Depiction of cell phase moisture transfer series. Reconfigured *Method of Cascading Weirs* [38, 39].

3.5. Stage 2: N Kinetic Transformations, Numerical Models

Not all node-sheds contain sources of sewage. The node-sheds that are flagged as sources are connected to the Wastewater-N Router function; the others by-pass this algorithm, routing only bulk recharge. This router is an algorithmic function, which arranges a series loop algorithm from cell 1 to *NCS* (specified number of cells in series), as the vadose water "cascades" through the router cells. The chemical reactions of ammonification, nitrification, and denitrification operate inside each cell, and the resulting concentration and effluent water is used as input into the next cell. As shown in Fig. 4, the algorithm operates on NCS, depending on the specified environmental conditions for the cell. The components in each cell, *J*, undergo an ordered preparation and process: (1) accounting for wastewater storage, output, field capacity; (2) preparation of storage constituents and mixed concentrations; (3) execution of chemical reactions and NH_3 NH_4^+ equilibrium; and (4) sorption of ammonia-N. These four processes are executed sequentially within each of the "cascading" cells and transferring N concentrations to the next cell, J.
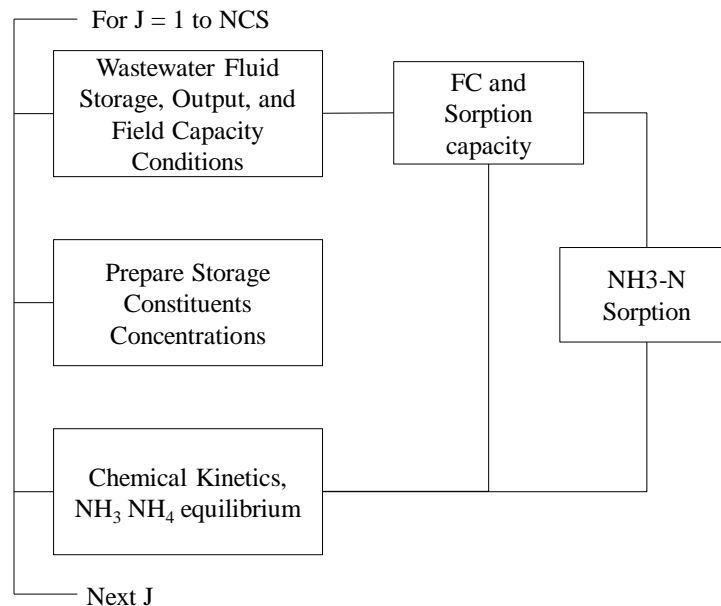
Figure 4. The general components in a wastewater-N router cell.

The Wastewater-N Router function begins as a flow router, preparing the node-shed parameter time constant factor. Its time in storage and number of phases are aligned with its respective node-shed slow flow router parameters. Then, it brings into the function the daily array values for organic-N, ammonia-N, DO, wastewater input volume, and meteoric dilution volume. Recall that these values were synthesized from the random discharge model. The wastewater volume is routed using slow flow parameters through each cell as was done in the flow router algorithm. In each cell however, the appropriate chemical processes are applied to the input constituents to calculate changes in concentration as the vadose water "cascades" through the cells.

3.5.1. Wastewater storage and routing

In this algorithm, wastewater is an input volume, I_2, along with meteoric dilution volume, D_2, into the first cell, $J = 1$. The final storage volume, S_2, is computed for the conditions dependent on cell J, Eq. 9. When cell $J > 1$, I_2 is output from the previous cell and there is no meteoric dilution volume. In the following equations, the subscripts (e.g. $j,2$) refer to the phase number ($J = j$) and time period, current (2) or previous (1), and $i2$ and $f2$ refer to current intermediate and final time period, respectively. Current intermediate time period means that the variable is undergoing updates in the phase subroutine, since the concentrations will undergo chemical kinetics within time in storage.

$$S_{j,2} = \begin{cases} S_{j,1} + I_{j,2} + D_{j,2} & J = 1 \\ I_{j,2} = O_{j-1,2} & J > 1 \\ S_{j,1} + I_{j,2} \end{cases}$$

Eq. 9

The field capacity of node-shed is the moisture limit that the bedrock material can hold against gravity. The field capacity of a node-shed cell phase is a rough estimate, using bedrock mass properties of cells to achieve a field capacity saturation effect. Field Capacity is estimated in Eq. 10, where $Dpth_{ns}$ is vadose depth at a node-shed, $sNOC$ is the number of router cells, A_{ns} is the area of the node-shed, ρ_{ns} is the bedrock density, φ_{ns} is the moisture capacity per bedrock mass.

$$FC_{ns} = \begin{cases} (Dpth_{ns} / sNPS) A_{ns} (1 - n_{ns}) \cdot \rho_{ns} \cdot \varphi_{ns} & \text{option true} \\ 0 & \text{option false} \end{cases}$$

Eq. 10

The field capacity for a wastewater sourced node-shed is $WFC = FC_{ns} \cdot A_{ww} / A_{ns}$, where A_{ww} is the specified effluent wetting area.

The option choice is cued to allow the simulation of a dry media which lets the modeler see the time for transfer and transport of wastewater and constituents, with the effect of field capacity. The alternate option signifies that the media field capacity is already filled and additional moisture just percolates through. When field capacity saturation is achieved, at all the phase cells, then that is when moisture can percolate through. The WFC_{wns} is the field capacity for the wastewater router, conditional with the field capacity option setting and cell phase moisture storage.

$$O_{j,2} = \begin{cases} 0 \\ \bar{I}_{j+1} = \dfrac{O_{j,1}}{2} \end{cases} \quad 0 \le S_{j,i2} \le WFC_{wns} \\ \begin{aligned} dQ_j &= \bar{I}_j - O_{j,1} \\ dQ_j \cdot C + O_{j,1} \\ S_{j,f2} - FC_{ns} \\ flag &= 1 \end{aligned} \quad 0 \le (S_{j,i2} - O_{j,i2}) \le WFC_{wns} \\ \bar{I}_{j+1,2} = \dfrac{(O_{j,1} + O_{j,2})}{2} \quad (S_{j,2} - O_{j,2}) > WFC_{wns} \end{cases} \quad S_{j,i2} > WFC_{wns}$$

Eq. 11

A flag condition of 1 is set for the given conditions above. The flag is used at the end of the phase after operations of the chemical kinetics to set the final volume. It is after the chemical kinetics because it is used as a divisor in determining a new constituent concentration, while summing the input mass and in phase mass. This flag is set to zero for every new phase, where $S_{j,f2} = S_{j,i2} - O_{j,2}$, otherwise $S_{j,f2} = WFC_{wns}$. It sets which formula to use to obtain the final storage before computing into the next phase.

3.5.2. Preparation of storage constituent concentrations

After wastewater storage volume has been accounted for, the mass per unit volume is calculated for each constituent input for the initial concentrations in solution. Equation 12 shows the phase condition formulas for organic-N (*RN*), ammonia-N (*AN*), nitrate-N (*NN*), and dissolved oxygen (*DO*). The concentration variables with initial *I* are input concentrations, respectively. The condition requires the cell (*J*) and current period storage (S_2). S_1 and I_2 are initial storage and current input volumes, respectively.

$$\begin{cases} RN_{1,i2} = \left(RN_{j,1} \cdot S_1 + IRN_{j,2} \cdot I_2\right)/S_2 \\ AN_{1,i2} = \left(AN_{j,1} \cdot S_1 + IAN_{j,2} \cdot I_2\right)/S_2 \\ NN_{1,i2} = \left(NN_{j,1} \cdot S_1 + INN_{j,2} \cdot I_2\right)/S_2 \\ DO_{1,i2} = \left(DO_{j,1} \cdot S_1 + IDO_{j,2} \cdot I_2\right)/S_2 \\ RN_{j,i2} = 0 : AN_{j,i2} = 0 : NN_{j,i2} = 0 : DO_{j,i2} = 0 \end{cases} \begin{array}{l} J = 1 \text{ or } S_2 > 0 \\ \\ \\ \\ J > 1 \text{ and } S_2 = 0 \end{array} \qquad \text{Eq. 12}$$

3.5.3. Chemical Kinetics of Ammonification, Nitrification, and Denitrification

The modeling of ammonification, nitrification, and denitrification requires careful programming for each phase of the wastewater-N router. The order is (1) oxidation of organic-N (ammonification); (2) oxidation of ammonia (nitrification, both nitrite and nitrate); and (3) reduction of nitrates (denitrification). This ordering does not imply that these reactions necessarily occur in series. Rather the appropriate reaction(s) must be invoked according to the conditions in each phase. The pivotal condition is the presence or absence of dissolved oxygen in the media, which determines whether or not nitrification proceeds. Similarly, denitrification requires an anoxic conditions and the presence of organic carbon.

Into each subsequent cell, the output of the previous phase becomes the input. The results of some of the reactions are time-dependent. The resulting concentrations of constituents are thus either limited by *time in storage*, *Ts*, or *time to consume dissolved oxygen* (*TDO*), which then continues into the next cell phase. Figure 5 provides the conceptual model of 3 conditions: $TDO \leq Ts$, $TDO > Ts$, and dissolved oxygen (*DO*) is continuously positive. For *DO* to be continuously positive, percolating water must gain and sustain oxygen throughout its vadose life. Assuming an ample amount of ammonia-N and the gain of *DO* upon discharge from septic or into sewage, nitrification will proceed. When $TDO \leq Ts$, then denitrification will occur in the phase within *Ts* time, but may not necessarily finish depending on the kinetics of denitrification. If $TDO > Ts$, then there will be left-over *DO*, which may promote nitrification into the next phases. Organic-N continues oxidation regardless of *DO*. When nitrification stops, ammonia-N concentration may become steady or continue to gain from convertible organic-N, assuming that organic-N is all convertible to ammonia-N. The production of nitrates is also limited by the available ammonia-N. Thus a special condition is made for ammonia-N as the limiting reagent.

The numerical solution is expressed in the following equations. Organic-N is oxidized, producing ammonia-N, using 1st order chemical kinetics: $RN_{j,f2} = RN_{j,i2} \cdot e^{-k_1 T_s}$ [46], where *RN* is organic-N, *k* is the exponential rate constant, and *Ts* is the time in storage variable described above. As also noted earlier, *j* is the cell of the series and *f* is the final process, and subscript 2 indicates the present time-step. The eventual chemical outcome in each phase depends on available quantities of constituents involved in the transformations.

The k_1 for ammonification or oxidation of organic-N is 0.110/hr [46]. The time variable is *Ts*, so it continues to decay throughout every phase of percolation. Assuming that *RN* is convertible, the ammonia-N produced is

$ANP = RN_{j,i2} - RN_{j,f2}$ in the phase. The ammonia-N undergoes equilibrium, assuming non-ionic ammonia that leaves as gas is quantified by Eq. 13.

$$AN_{j,ii2} = \left(AN_{j,i2} + ANP\right) - C_{mf}\left(AN_{j,i2} + ANP\right)$$

Eq. 13

The mole fraction of ammonia-N, C_{mf}, is determined by the equations derived from USEPA tables [36], dependent on mean monthly temperature and pH, Fig. 5. Temp (^{o}C)

Temp ºC	pH 7	pH 7.1	7.05 (avg)
20.0	0.396	0.498	0.447
20.5	0.410	0.516	0.463
21.0	0.425	0.535	0.480
21.5	0.441	0.555	0.498
22.0	0.457	0.575	0.516
22.5	0.474	0.596	0.535
23.0	0.491	0.617	0.554
23.5	0.509	0.640	0.575
24.3	0.527	0.663	0.595
24.5	0.546	0.687	0.617
25.0	0.566	0.711	0.639
25.5	0.586	0.737	0.662
26.0	0.607	0.763	0.685
26.5	0.628	0.790	0.709
27.0	0.651	0.818	0.735
27.5	0.674	0.846	0.760
28.0	0.697	0.876	0.787
28.5	0.722	0.907	0.815
29.0	0.747	0.938	0.843
29.5	0.772	0.970	0.871
30.0	0.799	1.000	0.900

Source: [36]
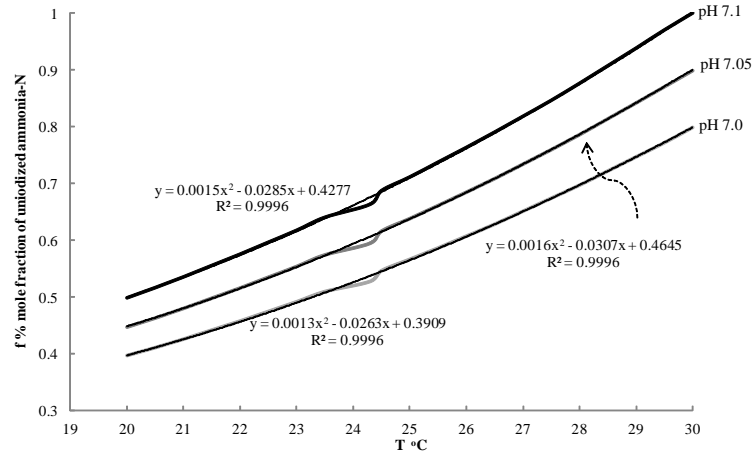
Figure 5. Mole fraction equations of unionized ammonia-N. Derived from [36].

The available ammonia-N that converts into nitrates is limited by the dissolved oxygen. The oxygen required for one nitrogen unit (from ammonia-N) to produce one nitrate unit is expressed in the chemical equation $2N + 3O_2 \xrightarrow{\text{nitrification}} 2NO_3^- + O_2 \xrightarrow{\text{nitrification}} 2NO_3^-$. The stoichiometric quantity of DO required for 1 mg/L of nitrogen to create nitrate is 4.57 mg/L of DO. Thus, the nitrate produced for the available DO (NDO) is expressed in $NDO = DO_{j,2}/4.57$. The resulting estimate of time to produce nitrates or time to consume DO (TDO) is shown in the expression, $TDO = NDO / k_3$, where $k_3 = 25$ ppm/hr [46]. For ammonia as a limiting reagent and stoichiometry of ammonia-N and nitrate-N is 1:1, the estimated time to consume ammonia into nitrates is derived from the 0th-order linear equation $t_{OA} = AN_{j,i2}/k_3$, solving for time.

For the case of continuous DO, assuming DO is never depleted, as in Cowan's lysimeter experiment [5, 48], and not a limiting reagent, *Nitrate-N* (*NN*) is produced from *ammonia-N* (*AN*) at the rate for each phase for the time in storage, *Ts*. The limiting reagent would then be ammonia-N, Eq. 14.

$$\begin{cases} \text{condition of continuous DO} \\ NN_{j,ii2} = k_3 \cdot Ts + N_{j,i2} \\ AN_{j,f2} = AN_{j,i2} - NN_{j,ii2} \big| AN_{j,i2} > NN_{j,ii2} \\ NN_{j,ii2} = AN_{j,i2} + N_{j,i2} \\ AN_{j,f2} = 0 \end{cases} \Big| AN_{j,i2} \le NN_{j,ii2}$$

Eq. 14

For limited DO, necessary defining conditions involve *TDO*, *Ts*, *AN*, and *NDO*. Equation 15 is the numerical solution dependent on time, available DO, and ammonia-N, conceptually depicted in Fig. 6.
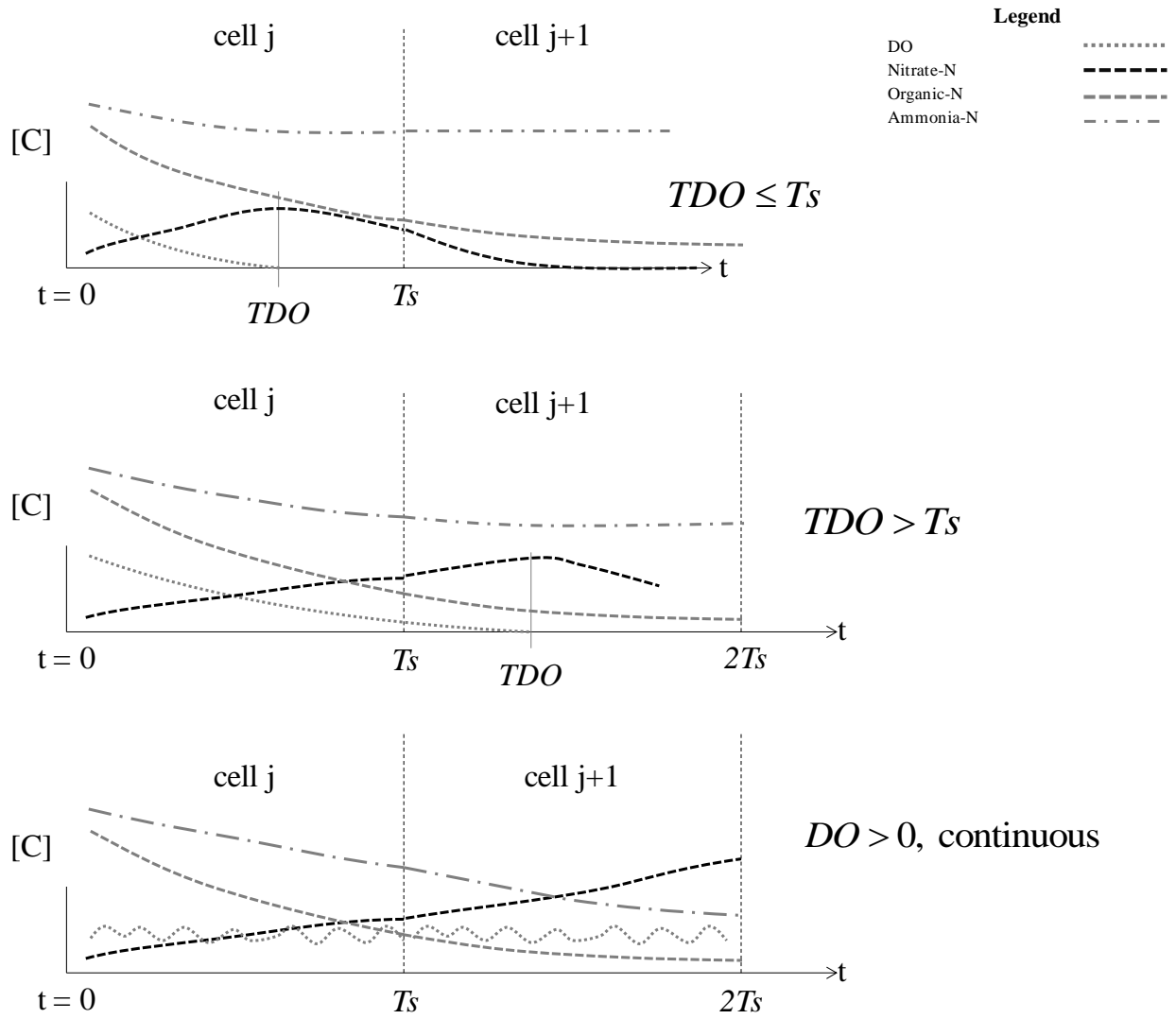
Figure 6. Time and constituent limits, conditions of chemical kinetics in a cell phase.

$$\begin{cases} \begin{vmatrix} t_{OA} = AN_{j,i2}/k_3 \\ N_{j,f2} = k_3 \cdot t_{OA} + N_{j,i2} \\ AN_{j,f2} = 0 \\ DO_{j,f2} = DO_{j,i2} - N_{j,f2} \cdot 3.42 \end{vmatrix} \quad 0 \le AN_{j,2} \le NDO \\ \begin{vmatrix} N_{j,f2} = k_3 \cdot TDO + N_{j,i2} \\ AN_{j,f2} = -k_3 \cdot T_S + AN_{j,i2} \\ DO_{j,f2} = 0 \\ N_{j,f2} = N_{j,f2} \cdot e^{-k_4(T_S - TDO)} \end{vmatrix} \text{denitrification option} \quad AN_{j,2} > NDO \end{cases} \quad TDO \le T_S$$

$$\begin{cases} \begin{vmatrix} NTS = k_3 \cdot T_S \\ t_{OA} = AN_{j,i2}/k_3 \\ N_{j,f2} = k_3 \cdot t_{OA} + N_{j,i2} \\ AN_{j,f2} = 0 \\ DO_{j,f2} = DO_{j,i2} - N_{j,f2} \cdot 3.42 \end{vmatrix} \quad 0 \le AN_{j,i2} \le NTS \\ \begin{vmatrix} N_{j,f2} = k_3 \cdot NTS + N_{j,i2} \\ AN_{j,f2} = -k_3 \cdot T_S + AN_{j,i2} \\ DO_{j,f2} = DO_{j,i2} - N_{j,f2} \cdot 3.42 \end{vmatrix} \quad AN_{j,2} > NTS \end{cases} \quad TDO > T_S$$

Eq. 15

For the case in which *DO* has been consumed, but in which the current period outflow is deemed as a percolate that gains *DO* into the next cell, a normal random generator for DO is set between 0.5 and 2 ppm of *DO*. Denitrification rate, k_4, is available in wastewater treatment studies [e.g., 23].

3.5.4. Sorption

As noted at the beginning, the primary geologic unit of the aquifer is the fine-grained foraminiferal Barrigada Limestone. Samples of this unit were used to develop empirical parameters by which to model N sorption reactions with the aquifer material. The mass of the sorbed phase may be estimated from the sorption isotherm of ammonia-N and Barrigada Limestone. The Langmuir model [15] is expressed:

$$q = a \frac{K_L C_e}{(1 + K_L C_e)},$$
Eq. 16

where q is the mass sorbate per mass sorbent, *a* is the sorbate saturation limit per unit mass of sorbent (mass/mass), K_L is the Langmuir constant (volume/mass), and C_e is the equilibrium concentration.

A batch equilibrium test was performed by Habana and Rouse using spectral analysis to estimate the sorption characteristics. The maximum mass sorbed was 2.52 μg/g, rounded to 3 μg/g. At low concentrations, graph of *q* vs. *Ce* are nearly linear [15], so that the Langmuir constant may be approximated by linear regression using the inverse form of the Langmuir model (Fig. 7). K_L is about 0.005 L/μg.

Ce (µg/L)	q (µg/g)	Ce(a-q) (µg/L . µg/g)	KL (L/µg)
22	0.3	59	0.0056
43	0.4	110	0.0040
59	0.7	136	0.0051
81	0.8	176	0.0046
101	1.0	205	0.0047
130	0.8	282	0.0029
136	1.4	216	0.0065
162	1.4	265	0.0052
		average =	0.0048
		geomean =	0.0047

y = 65.975x + 0.3333
R² = 0.9145

(chart: 1/q vs 1/Ce)
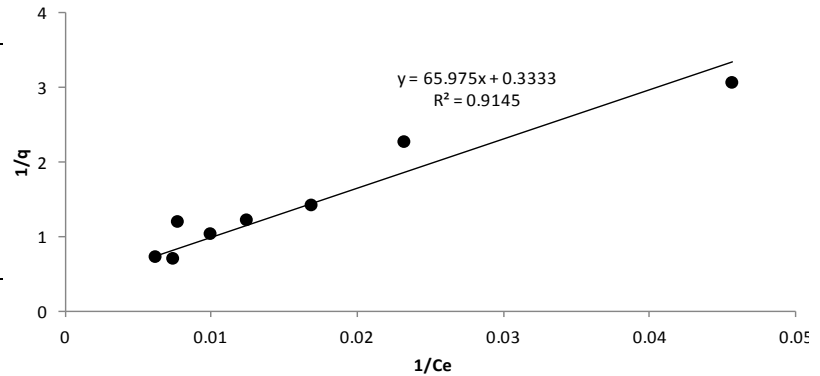
Figure 7. Linear form of Langmuir sorption analysis of ammonia-N and Barrigada Limestone.

The equilibrium concentrations were obtained using the Langmuir formula and linear regression analysis for the initial concentration conditions:

$$\begin{cases} AMN_{j,2eq} = 0.9858 \cdot AMN_{j,i2} \big| 0 \le AMN_{j,i2} \le 10 \\ AMN_{j,2eq} = AMN_{j,i2} - 0.0984 \big| AMN_{j,i2} > 10 \end{cases} \qquad \text{Eq. 17}$$

Sorption is modeled for all the ammonia-N phase by the Langmuir isotherm. The Langmuir equation, as mass of sorbate per mass of sorbent, requires an estimate of mass in the reaction in order to determine the maximum sorption of ammonia-N. The volume of the water in each cell is estimated using the depth of the node-shed, from surface to water table, divided by the slow flow number of cells for the router setting at that node-shed. The mass of the porous media bedrock of a wastewater node-shed cell (Kg) is solved using $\theta = V(1-n)\rho$, where V is volume of phase cell, n is porosity, and ρ is the bedrock density (2210 Kg/m^3). The maximum amount of ammonia-N mass that can be sorbed is solved by the product of a and θ, converted to grams:

$$a\theta \cdot 10^{-3} \frac{g^2}{\mu g \cdot Kg} = \text{ maximum mass of ammonia-N that can be sorbed (g)} \qquad \text{Eq. 18}$$

Likewise, the mass of ammonia-N sorbed is solved by:

$$q_2\theta \cdot 10^{-3} \frac{g^2}{\mu g \cdot Kg} = \text{mass of sorbed ammonia-N (g)}. \qquad \text{Eq. 19}$$

A sorption variable, *sorp*, is used to account sorption accumulation and limited by $Sorp_{max}$ – from Eq. 18. The numerical model for sorption is:

$$\begin{cases} AMNex_{j,2} = sorp_1 + \dfrac{q_2\theta}{1000} - sorp_{max} \\ sorp_2 = sorp_{max} \\ AMNout = \dfrac{AMN_{j,2eq} \cdot S_2 + AMNex_{j,2}}{S_2} \end{cases} \Bigg| sorp_1 + \dfrac{q_2\theta}{1000} > Sorp_{max}$$

$$\begin{cases} sorp_2 = sorp_1 + \dfrac{q_2\theta}{1000} \\ AMNout = AMN_{j,2eq} \end{cases} \Bigg| sorp_1 + \dfrac{q_2\theta}{1000} \le Sorp_{max} \qquad , \qquad \text{Eq. 19}$$

where *AMNex* is the excess mass of ammonia-N. Excess occurs when the sorption containment variable plus the current sorption mass calculated is greater than the maximum sorption. The *ammonia-N output AMNout* of phase j, input to phase j+1, as concentration, is the equilibrium mass plus excess mass divided by the wastewater storage.

4. RESULTS AND DISCUSSION

The model domain is prepared in ESRI® ArcMap, Geographic Information System, similar to preparation in [8, 9], adding attributes of Landcover (Guam Bureau of Statistics and Plans), Soils [40], and Sewer Status Survey Map (Water Environmental Research Institute, Guam EPA, and Guam Waterworks Authority). Temporal data, daily rainfall and pan evaporation, were from 1982 to 1985 [27]. The domain has more than 100 node-sheds and 41 effluent sources. Stage 1 daily simulation values extracted from selected source assigned node-shed 18 are displayed for results in Figs. 8-11. In Fig. 8, the top chart is the intercept and soil moisture model results and bottom chart is synthesized wastewater and constituent discharge. The Intercept and soil moisture shows the input rainfall and pan evaporation data (in) on the secondary axis and soil moisture, daily moisture to recharge, evapotranspiration, and sum of intercept evaporation and evapotranspiration (total evaporation) in m^3 in the primary axis. The bottom chart is the synthesized daily discharge of wastewater and N constituents. The primary axis shows the wastewater volume (m^3) and the secondary axis shows the constituents (ppm): ammonia-N, Organic-N, and DO.

The Stage-2 bulk node-shed meteoric recharge has the daily rain data (in) in the secondary axis and the fast, slow, and total recharge (m^3) in the primary axis, Fig. 9. The chart shows the time distribution of rainfall to recharge at node-shed 18. The addition of intercept into the model significantly reduces the moisture input and the moisture to flow to recharge, compared to the previous model with no intercept [8, 9]. In Fig. 8, small rainfall in the dry season of less than pan evaporation and field capacity does not make it past the soil model as moisture to recharge. Between March to mid May, there is no meteoric recharge (Fig. 9). Figure 10 shows greater concentration levels of N species that are transported during the dry season and most diluted following soon after the peaks of the rainy season.

Figure 10 shows the fate and transport of wastewater and N solutes through a continuous DO scenario, recall Fig. 1. The top chart has the transported wastewater (m^3), transported nitrate-N (ppm), and transported organic-N (ppm) in the primary axis, and input ammonia-N (ppm, source discharge) and transported ammonia-N (ppm) in the secondary axis. The continuous DO scenario produced and transported about 6 ppm of nitrates, which was chosen as a test to produce a selected quantity. The production of nitrates is limited by the transformable ammonia-N, available DO, and the final route cell reach. Adding more cells would increase the production of nitrates as long as there is ammonia-N present in each cell it cascades into. Notice the starting ammonia-N and the remaining ammonia-N, a result of the transport and transformation process. The dilution from meteoric recharge is also effective, but attenuates with increased number of cells in the router. Aligning Figure 9 to Figure 10, the recharge responses are followed by reduced concentrations, an effect of dilution. Convertible organic-N is nearly completely transformed into ammonia-N. The bottom chart shows the transported total N (ppm) in the secondary axis and transfer of wastewater volume (ppm) in the primary axis. The transferred wastewater is attenuated compared to its discharge input. The test output provided applied 25 routing cells. Increasing the number of routing cells result in smoothening and "leveling out" the curves.

Scenario 1 (see Fig. 1) transport is percolation and consumed DO. When nitrates exist and DO is very low, nitrates are denitrified. Figure 11 shows the results for such a case where transported nitrate-N concentrations are very low. The model simulates a single aeration of effluent upon discharge; the DO is consumed to make nitrates from ammonia-N and the produced nitrates are denitrified throughout its fate through the vadose. Had there been more cells added in the routing parameter for this node-shed, denitrification would have more time to deplete more nitrates.

VADOCHARGE-N is designed to be spatially variable and uniquely parameterized in each node-shed. The limits are available data, definitely improved with more input and monitoring data. The difficulty with uplifted karst is borehole exploration is discouragingly costly ($300/ft or ~$1,000/m). Monitoring stations are carefully selected and usually placed in unused or abandoned well sites. Currently, there are less than 15 observation wells and may be too remote from a domain of interest. However, this model establishes grounds for recommending increased monitoring and data collection, a much needed requirement for any model in pursuit of accuracy.

A deep vadose karstic system such as the NGLA, Guam's most valuable renewable water source, requires many ways to assess quality due to the complex hydrogeology. The goal of VADOCHARGE-N is to simulate the domestic sewage discharge impact and to suggest civil development regulation above the water resource. VADOCHARGE-N provides a means to estimate and adequately visualize impact of civil development high above the water source. With a continuously developing vadose model, as this VADOCHARGE-N, now including domestic sewage contaminant transport, local water protection and production agencies can include this model to make improved sustainable management decisions and optimize development practices.
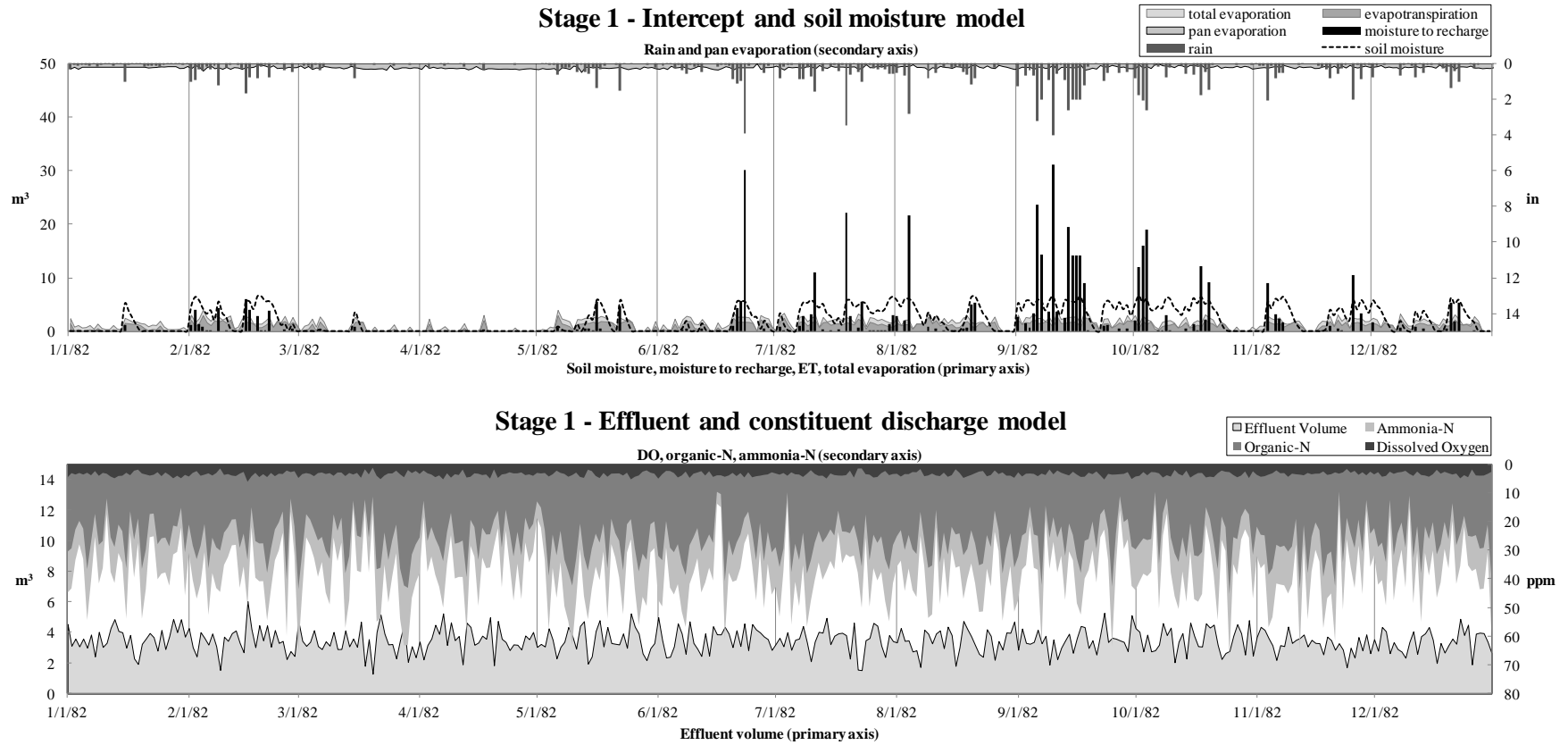
Figure 8. Stage-1, selected effluent source node-shed 18, sample of soil moisture and discharge model results.
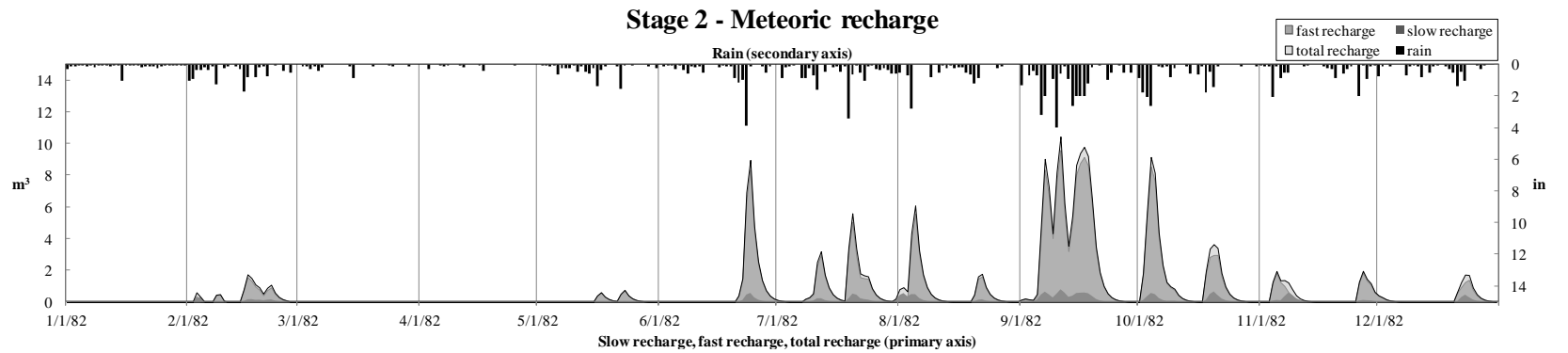
Figure 9. Stage 2, meteoric recharge hydrograph of a selected node-shed.
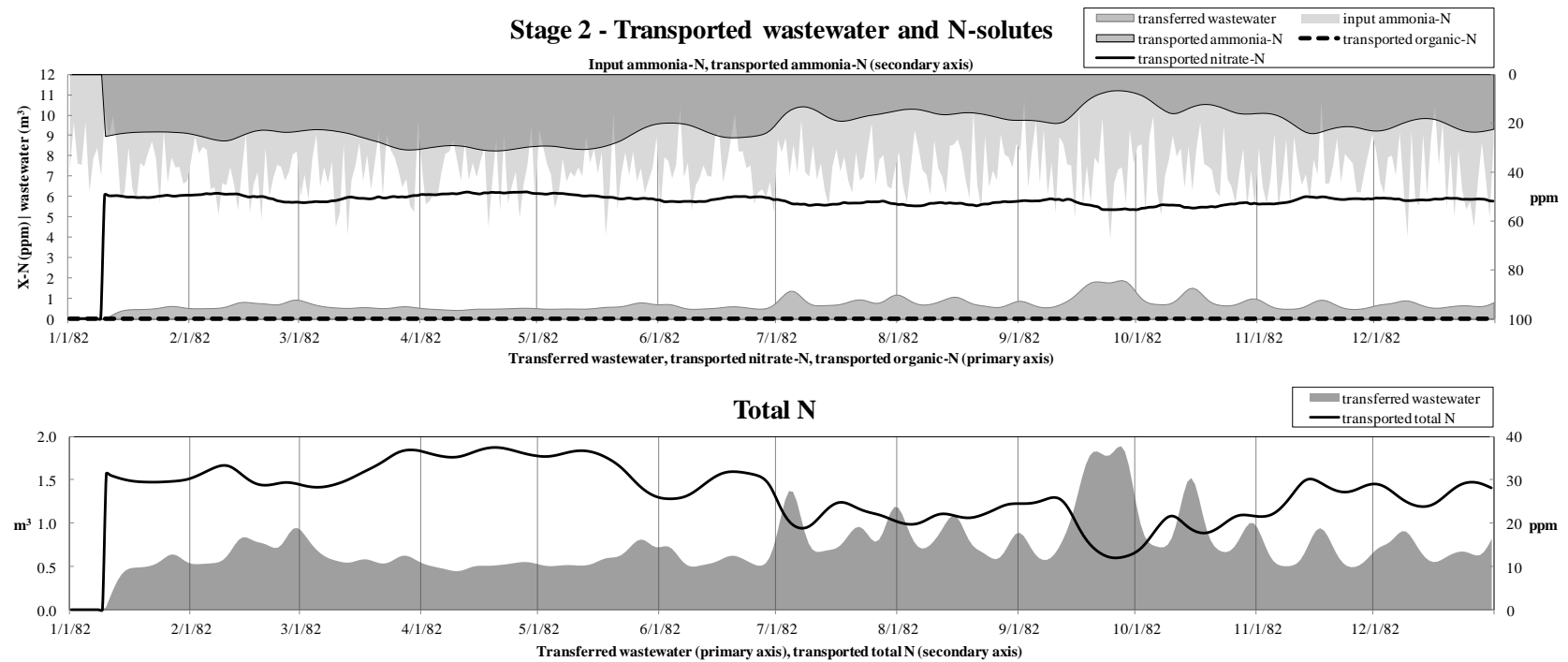
Figure 10. Scenario 1, DO is continuous. Top chart shows transfer of wastewater and transport of nitrate-N, organic-N, and ammonia-N.
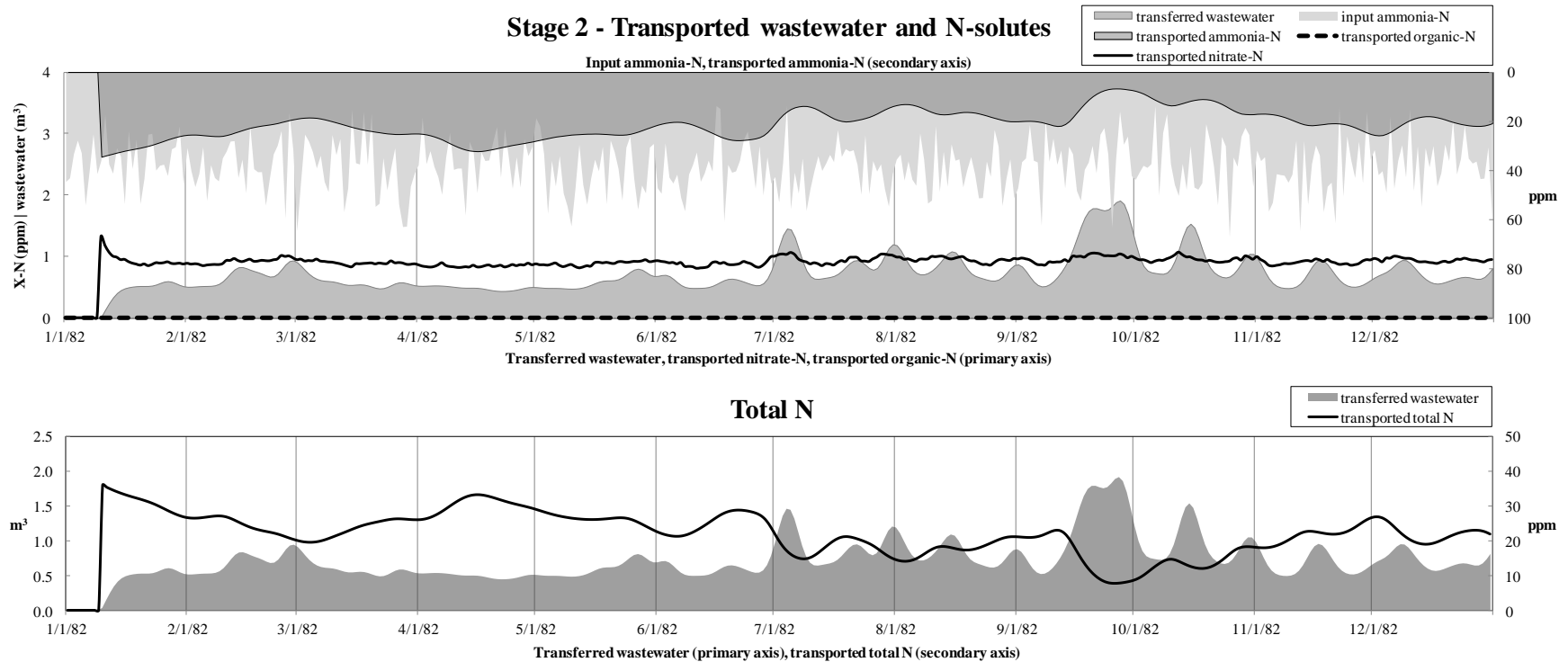
Figure 11. Scenario 2, DO is consumed. When DO is consumed in the percolation, denitrification prevails, thus the lower concentration of nitrate-N transported.

5. CONCLUSION, SUMMARY AND RECOMMENDATIONS FOR FUTURE RESEARCH

This modeling effort brings sustainable development practice into the frontiers of environmental research technology for Guam. VADOCHARGE-N is a comprehensive vadose flow and N transport model, simulating the percolation and simultaneous N cycle to reach the water table. The detailed description of the numerical model provided is the heart of the computer program development and design. The model is robust and parameters are spatially assignable for each node-shed in the domain for adjusting and making history matching. Developed in Excel, it is easy to distribute and modify when necessary, affordable, and easy to upgrade, and it is not vulnerable to numerical instabilities as standard numerical models can be.

The model should next be tested in field trials against water samples and lysimeter data. Calibration is made matching hydrograph and transport results with field data, adjusting Ts and NCS to obtain appropriate attenuation and lag respectively. Future applications of the model should be done with it coupled to a dual-phase phreatic contaminant model such as the USGS's SUTRA (Saturated-Unsaturated Transport). This model may be used to elucidate and anticipate potential subsurface contamination vulnerabilities and impact. This is important for determining the current state of development as well as future buildup, considering alternatives and improvement to wastewater disposal [1]. When coupled to a phreatic flow and transport model, finite element or finite difference methods, the results may provide insight to the extent of sewage discharge impact, suggesting necessary control and regulation practices. It was practically designed to determine the limits to development density and capacity, with respect to water quality regulations.

6. ACKNOWLEDGEMENTS

REFERENCES

[1] Bauer DH, Conrad ET, Sherman DG (1979). Evaluation of On-Site Wastewater Treatment and Disposal Options. US Environmental Protection Agency, Ohio.

[2] Bear J (1972). Dynamics of Fluids in Porous Media. 2nd Printing 1975, American Elsevier Publishing Company, Inc., New York.

[3] Canter LW, Knox RC (1995). Septic Tank System Effects on Ground Water Quality. Lewis Publishers, Inc., Michigan.

[4] Contractor DN, Jenson JW (2000). Simulated effect of vadose infiltration on water levels in the Northern Guam Lens Aquifer. Journal of Hydrology 229:232-254.

[5] Cowan PA, Clayshulte RN (1980). Laboratory Application of secondary Sewage Effluent to Argillaceous Limestone, Technical Report (TR) 18. Water and Environmental Research Institute, (WERI) of the Western Pacific[1], University of Guam (UOG), Mangilao, Guam.

[6] Datuin TH, Lander MA, Olsen AE, Jenson JW (2010). Statistical Analysis of Recharge, Master Thesis, WERI, UOG, Mangilao, GU.

[7] Fiering B, Jackson B (1971). Synthetic Streamflows, Vol. 1. Water Resources Monograph, Washington, D.C.

[8] Habana NC, Heitz LF, Olsen AE, Jenson JW (2009). Vadose flow synthesis for the Northern Guam Lens Aquifer. TR 127, WERI[1], UOG, Guam.

[9] Habana NC, Heitz LF, Olsen AE, Jenson JW, Salvacion JL (2013). VADOCHARGE: Groundwater Recharge Model for an Uplifted Island karst Aquifer, Guam, USA. International Journal of Environmental Engineering Science and Technology Research 1(8):141-164.

[10] Huntoon PW (1995). Is it appropriate to apply porous media groundwater circulation models to karstic aquifers?, *in* Aly El-Kadi ed., Groundwater Models for Resources Analysis and Management: Boca Raton, FL. Lewis Publishers, 339-358.

---

[1] www.weriguam.org

[11]   Johnson RL, Palmer CD, Fish W (1989). Chapter 5: Subsurface chemical processes, Seminar Publication, Transport and Fate of Contaminants in the Subsurface. USEPA.

[12]   Jocson JMU, Contractor D, Jenson JW (1999). Numerical Modeling and Field Investigation of Infiltration, Recharge, and Discharge in the Northern Guam Lens Aquifer. TR 88, WERI[1], UOG, Guam (1999).

[13]   Jocson JMU, Jenson JW, Contractor DN (2002). Recharge and aquifer response: Northern Guam Lens Aquifer, Guam, Mariana Islands. Journal of Hydrology 260:231-254.

[14]   Klimchouk AB, Ford DC, Palmer AN, Dreybrodt W (2000). Speleogenesis: Evolution of Karst Aquifers. National Speleological Society, Alabama.

[15]   Knox RC, Sabatini DA, and LW Canter (1993). Subsurface Transport and Fate Processes, Lewis Publishers, CRC Press, Inc., Florida.

[16]   Konikow LF (2011). The secret to successful solute–transport modeling. Ground Water 49(2):144-159.

[17]   Leibundgut C (1998). Vulnerability of karst aquifers. Karst Hydrology (Proceedings of Workshop W2), Rabat, Morocco, April-May 1977, IAHS 247:45-60.

[18]   Lander MA, Jenson JW, Beausoliel C (2001). Responses of Well Water Levels on Northern Guam to Variations of Rainfall and Sea Level. TR 94, WERI[1], UOG, Mangilao, Guam USA. www.weriguam.org

[19]   Lander MA (1994). Meteorological Factors Associated With Drought on Guam. TR 75, WERI[1], UOG, Mangilao, Guam USA.

[20]   Lander MA (2008). Personal Communications, Professor of Meteorology, WERI[1], UOG, Mangilao, Guam USA.

[21]   Matson E (1993). Nitrification in Guam's Soils and Sediments. TR 71, WERI[1], UOG, Mangilao, Guam USA.

[22]   Matson, E, Denton GRW (2010) Personal communications, Professors at Marine Laboratory and WERI, respectively. UOG, Mangilao, Guam USA.

[23]   Metcalf, Eddy, Tcholbanoglous G, Burton FL (1991). Wastewater Engineering: Treatment, Disposal, and Reuse. 3rd Edition, McGraw Hill, New York.

[24]   McDonald MQ (2002). Nitrate-nitrogen Concentrations in the Northern Guam Lens and Potential Nitrogen Sources. TR 95, WERI[1], UOG, Mangilao, Guam USA.

[25]   Moran D, Jenson JW (2004). Dye Trace of Groundwater Flow from Guam International Airport and Harmon Sink to Agana Bay and Tumon Bay, Guam. TR 97, WERI[1], UOG, Mangilao, Guam USA.

[26]   Mylroie, JE, Jenson JW (2000). The Carbonate Island Karst Model applied to Guam. Theoretical and Applied Karstology 13(14):51-56.

[27]   National Climatic Data Center (NCDC) (2010). Climatedata[TM] Vol. 22.3 and Hydrodata[TM]. Vol. 23.3, Hydrosphere Data Products (Compact Disk Program Set).

[28]   New Hampshire Department of Environmental Services (NHDES) (2006). WD-DWGB 3-9 2010, Nitrate and Nitrite: in Drinking Water. NHDES, New Hampshire. http://des.nh.gov/organization/commissioner/pip/factsheets/dwgb/ (as of 2013)

[29]   Palmer AN, Palmer MV, Sasowski ID (1999). Karst Modeling. Karst Waters Institute, Special Publication 5:146-157.

[30]   Pacific ENSO Applications Climate Center (PEAC) (2011). Pacific El Nino Southern Oscillation (ENSO) update, 17(3):1-11.

[31]   Press WH, Flannery BP, Teukolsky SA (1992). Numerical Recipes in FORTRAN 77 Vol 1: The Art of Scientific Computing. 2nd edition, Cambridge University Press, USA.

[32]   Rotzoll K, Gingerich SB, Jenson JW, el-Kadi AI (2013). Estimating hydraulic properties from tidal attenuation in the Northern Guam Lens Aquifer, territory of Guam, USA, Hydrogeology Journal 21:643-654.

[33]   Senarath DCH (1987). Two case studies in estimation of groundwater recharge, groundwater monitoring and management. Symposium on Ground Water Monitoring and Management, Dresden, Germany, March 1987.

[34]   Singh VP (1995). Computer Models of Watershed Hydrology. Water Resources Publications, LLC, Colorado, USA.

[35]   Singh VP, Donald FK (2002). Mathematical Models of Small Watershed Hydrology and Applications. Water Resources Publications, LLC, Colorado, USA.

[36]   Thurston RV, Russo RC, Emerson K (1979). Aqueous Ammonia Equilibrium - Tabulation of Percent Un-ionized Ammonia, Environmental Research Laboratory - Duluth, USEPA, Minnesota.

[37]   Tracey JI, Schlanger SO, Stark JT, Doan DB, May HG (1964). General Geology of Guam: Geology and Hydrology of Guam, Mariana Islands. Geologic Survey Professional Paper 403(A), US Department of Interior, USGS, USA.

[38] US Army Corps of Engineers (USACE) (1994). Flood-Runoff Analysis, Ch. 9: Streamflow and Reservoir Routing. Department of the Army, US Army Corps Engineers (USACE), Washington, D.C.

[39] USACE – North Pacific Division (NPD) (1987, 1989) User's Manual: Microcomputer Version of the Streamflow Synthesis and Reservoir Regulation (SSARR) Model, draft as of 1987, draft as of 1989, USACE-NPD, Oregon.

[40] US Department of Agriculture (USDA), Natural Resource Conservation Service (NRCS; formerly Soil Conservation Service, SCS) (1988). Soil Survey of the Territory of Guam. National Cooperative Soil Survey, USDA, NRCS (SCS), University of Guam, and Department of Commerce, Guam, USA.

[41] US Environmental Protection Agency (USEPA) (1978). Guam: sole or principle source aquifer designation, Federal Register 43, FR 17888.

[42] USEPA (1989). Seminar Publication: Transport and Fate of Contaminants in the Subsurface. USEPA, Center for Environmental Research Information, Ohio.

[43] Vacher, HL, and JE Mylroie (2002) Eogenetic karst from the perspective of an equivalent porous medium. Carbonates and Evaporites 17:182-196.

[44] Ward AD, Trimble SW (2004). Environmental Hydrology. 2nd edition, CRC Press LLC, Lewis Publishers, Washington D.C.

[45] White WB (2003). Conceptual models for karstic aquifers. Speleogensis and Evolution of Karst Aquifers 1:1-6.

[46] Wong-Chong, GM, and RC Loehr (1975). The kinetics of microbial nitrification. Water Research 9:1099-1106.

[47] Worthington SRH (2003). A comprehensive strategy for understanding flow in carbonate aquifer. Karst Modeling, Special Publication 5:8.

[48] Zolan, W J, Clayshulte, RN, Winter SJ (1978). Urban Runoff Pollutant Adsorption and Filtering by Selected Northern Guam Soil and Limestone. Water Resources Research Center (WERI's former name)[1], UOG, Mangilao, Guam USA.